7th International Conference on Mechanical Engineering 2010 (Gépészet 2010)
Budapest, 25-26. May 2010.
ISBN 978-963-313-007-0

COMPUTED TORQUE CONTROL OF UNDER-ACTUATED DYNAMICAL SYSTEMS MODELED BY NATURAL COORDINATES

Ambrus Zelei [1]
zelei.ambrus@gmail.com

László L. Kovács
HAS-BUTE Research Group on Dynamics of Machines and Vehicles
H-1111, Budapest, Muegyetem rkp. 3-5. kovacs@mm.bme.hu

László Bencsik [1]
l.bencsik@hotmail.com

Gábor Stépán [1]
stepan@mm.bme.hu

[1] Department of Applied Mechanics, Budapest University of Technology and Economics
H-1111, Budapest, Muegyetem rkp. 5.

Abstract: *The under-actuated systems have less control inputs than degrees of freedom. We assume that the investigated under-actuated systems have desired outputs of the same number as inputs. In spite of the fact that the inverse dynamical calculation leads to the solution of a system of differential algebraic equations (DAE), the desired control inputs can be determined uniquely by the method of computed torques.*

We often use natural (Cartesian) coordinates to describe the configuration of the robot, while a set of algebraic equations represents the geometric constraints. In this modeling approach the mathematical model of the dynamical system itself is also a DAE.

The method of computed torque control with a PD controller is applied to under-actuated systems described by natural coordinates. The inverse dynamics is solved via the backward Euler discretization of the DAE system for which a general formalism is proposed. Some results are presented in the form of a case study for a cart-pole system and confirmed by numerical simulation.

Keywords: *computed torque control, under-actuated, differential-algebraic equations.*

1. INTRODUCTION

This paper proposes a generalized formalism for the computed torque control of under-actuated dynamical systems with geometric constraints and prescribed servo constraints.

The under-actuated dynamical systems have less control inputs than degrees of freedom. Typical examples of under-actuated systems involve the unmanned air vehicles, underwater vehicles, wheel driven mobile robots (see Fig.1./a). The elastic behavior of the components of the controlled dynamical system may cause the problem of under actuation [6]. On Fig.1./b we can see a motor and a rotor connected by an elastic shaft, where we can approximate the elastic shaft with a massless torsional spring element. Cranes (see fig.1./c) are also under-actuated because there is not direct action on the payload position. The crane-like robot manipulator developed on the ACROBOTER project [4, 7] also has more DoFs than control inputs. The structure of the robot is shown in Fig.1./d. The system connects to the ceiling based anchor point system (AP). The climber unit (CU) is able to move on the anchor points. A windable main cable hangs down from the CU and connects to three windable secondary cables via the cable connector (CC). The three secondary cables orienting the swinging unit (SU), in which a gripper and most of the sensors can be found. The number of DoFs is 12 and the number of actuators is 10 including the ducted fan actuators of the swinging unit and the cable winding mechanisms.

7th International Conference on Mechanical Engineering 2010 (Gépészet 2010)
Budapest, 25-26. May 2010.
ISBN 978-963-313-007-0

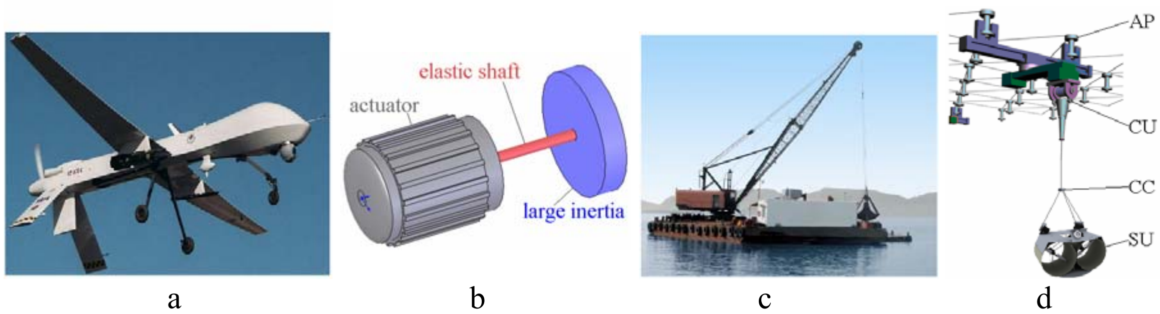

Fig.1. Under-actuated systems: unmanned air vehicle (a), elastic shaft (b), crane (c) and ACROBOTER (d)

In this work we assume that the system has desired outputs of the same number as control inputs. The servo constraints define the desired system outputs accordingly to the task. In spite of the fact that the inverse dynamical calculation leads to the solution of a system of differential algebraic equations (DAE), the desired control inputs can be determined uniquely by the computed torque method generalized for under-actuated systems.

Several dynamical systems, especially robots with parallel kinematic chains have a complex dynamics, which may hardly be modeled using conventional robotic approaches. An alternative modeling technique is to use natural (Cartesian) coordinates to describe the configuration of the robot. The number of descriptor coordinates is larger than the DoFs thus a set of algebraic equations represents the geometric constraints. In this approach the dynamics of the controlled system is modeled by a DAE.

The generalization of computed torque control for under-actuated systems is discussed in [8]. The method called CDCTC (computed desired computed torque control) can be applied only for systems that are represented by minimum number generalized coordinates $\overline{\mathbf{q}}$, and the mathematical model is an ODEs:

$$\mathbf{M}(\overline{\mathbf{q}})\ddot{\overline{\mathbf{q}}} + \mathbf{f}(\overline{\mathbf{q}}, \dot{\overline{\mathbf{q}}}, t) = \mathbf{Hu}\,, \tag{1}$$

where $\mathbf{M}$ is the mass matrix, $\mathbf{f}(\overline{\mathbf{q}}, \dot{\overline{\mathbf{q}}}, t)$ represents the external and internal forces except the control forces, $\mathbf{H}$ is the input matrix and $\mathbf{u}$ is the input vector. The phrase "computed desired" means that the uncontrolled coordinates cannot be arbitrarily prescribed but they can be calculated from the internal dynamics of the controlled system. Contrarily the controlled coordinates are prescribed and the control law that eliminates the error of the controlled coordinates at $t \to \infty$ is:

$$\mathbf{Hu} = \mathbf{M}(\overline{\mathbf{q}}^d)\ddot{\overline{\mathbf{q}}}^d + \mathbf{f}(\overline{\mathbf{q}}^d, \dot{\overline{\mathbf{q}}}^d, t) + \mathbf{K}_P(\overline{\mathbf{q}}^d - \overline{\mathbf{q}}) + \mathbf{K}_D(\dot{\overline{\mathbf{q}}}^d - \dot{\overline{\mathbf{q}}})\,, \tag{2}$$

where $\mathbf{K}_P$ and $\mathbf{K}_D$ are the gain matrices of the linear compensator. Equation (2) has to be solved for the control input $\mathbf{u}$ and for the uncontrolled subset of generalized coordinates $\overline{\mathbf{q}}$. The basic idea is to use the null space $\mathbf{N}$ of the input matrix $\mathbf{H}$ to project the equations into the space of the uncontrolled motion (3). The projected system can be solved for the uncontrolled coordinates. If we know the uncontrolled coordinates, the control inputs can be determined by equation (4).

$$\mathbf{0} = \mathbf{N}^{\mathrm{T}}\left[\mathbf{M}(\overline{\mathbf{q}}^d)\ddot{\overline{\mathbf{q}}}^d + \mathbf{f}(\overline{\mathbf{q}}^d, \dot{\overline{\mathbf{q}}}^d, t) + \mathbf{K}_P(\overline{\mathbf{q}}^d - \overline{\mathbf{q}}) + \mathbf{K}_D(\dot{\overline{\mathbf{q}}}^d - \dot{\overline{\mathbf{q}}})\right] \tag{3}$$

$$\mathbf{u} = \left(\mathbf{H}^{\mathrm{T}}\mathbf{H}\right)^{-1}\mathbf{H}^{\mathrm{T}}\left[\mathbf{M}(\overline{\mathbf{q}}^d)\ddot{\overline{\mathbf{q}}}^d + \mathbf{f}(\overline{\mathbf{q}}^d, \dot{\overline{\mathbf{q}}}^d, t) + \mathbf{K}_P(\overline{\mathbf{q}}^d - \overline{\mathbf{q}}) + \mathbf{K}_D(\dot{\overline{\mathbf{q}}}^d - \dot{\overline{\mathbf{q}}})\right] \tag{4}$$

It is possible to adopt the CDCTC method for natural coordinate based system, which is described by a redundant set of descriptor coordinates $\mathbf{q}$ and the equations of motion constitute a DAE. The solution requires an additional projection [5] that results an ODE. After the projection the CDCTC method can be applied, but it may be computationally too expensive because of the repeated projections.

Instead of the application of the CDCTC method we solve the inverse dynamic problem via the backward Euler discretization of the DAE system. The backward method requires the solution of a system of nonlinear algebraic equations in each time step, which is solved by

Newton-Raphson iteration. A general formalism is proposed for the analytical calculation of the Jacobian of the Newton-Raphson method.

The results are presented in the form of a case study for a cart-pole system and confirmed by numerical simulation. The numerical results are compared with analytical calculations.

2. PROBLEM FORMULATION

By using the redundant set of descriptor coordinates $\mathbf{q}$ the equation of motion, the geometric constraint vector of the system and the servo constraint vector can be written as:

$$\mathbf{M}\ddot{\mathbf{q}} + \mathbf{\Phi}_{\mathbf{q}}^{\mathrm{T}}(\mathbf{q})\boldsymbol{\lambda} = \mathbf{Q}_g + \mathbf{H}(\mathbf{q})\mathbf{u}\,, \tag{5}$$

$$\boldsymbol{\varphi}(\mathbf{q}) = \mathbf{0}, \tag{6}$$

$$\boldsymbol{\varphi}_s(\mathbf{q}, \mathbf{p}(t)) = \mathbf{0}. \tag{7}$$

Equation (5) is the Lagrangian equation of motion of the first kind, where $\mathbf{M}$ is the $n \times n$ sized constant matrix [1]. Symbol $\mathbf{Q}_g$ is the generalized gravity force. The m number of geometric constraints are represented by the vector $\boldsymbol{\varphi}(\mathbf{q})$ in (6) and $\mathbf{\Phi}_{\mathbf{q}}(\mathbf{q})$ is the Jacobian matrix of the constraints. The corresponding Lagrangian multipliers are denoted by $\boldsymbol{\lambda}$. The l dimension input vector is $\mathbf{u}$ and the $n \times l$ sized $\mathbf{H}(\mathbf{q})$ is the generalized input matrix.

The number l of the control inputs is less than the $n - m$ DoFs of the system, thus it is under-actuated. The task of the robot is formulated by the servo-constraint vector $\boldsymbol{\varphi}_s(\mathbf{q}, \mathbf{p}(t))$ [3, 6] given in equation (7). The dimension of the servo-constraint vector is also l that means the l number of control inputs can uniquely be determined.

The servo constraints depend on the function $\mathbf{p}(t)$ that can be handled as the desired system output and it may describe the desired trajectory of a certain point and/or the desired orientation of the end-effector. The servo-constraints can be formulated as:

$$\boldsymbol{\varphi}_s(\mathbf{q}, \mathbf{p}(t)) = \mathbf{h}(\mathbf{q}) - \mathbf{p}(t)\,, \tag{8}$$

where $\mathbf{h}(\mathbf{q})$ gives the prescribed system outputs as the function of the descriptor coordinates. We assume that the servo-constraints and a well chosen subset of geometric constraints can be solved for the controlled coordinates $\mathbf{q}_c$ in closed form. Than the task can be defined by $\mathbf{q}_c = \mathbf{q}_c^d$, where the superscript d refers to the desired value. Important to notice that the computed torque control method by direct discretization does not require to use $\mathbf{q}_c = \mathbf{q}_c^d$, because the direct discretization can handle the full constraint system composed by $\boldsymbol{\varphi}(\mathbf{q})$ and $\boldsymbol{\varphi}_s(\mathbf{q}, \mathbf{p}(t))$, but the size of the system increases.

For the partitioning of the descriptor coordinates we introduce the vector of controlled coordinates with $\mathbf{q}_c = \mathbf{S}_c^{\mathrm{T}}\mathbf{q}$ and $\mathbf{q}_u = \mathbf{S}_u^{\mathrm{T}}\mathbf{q}$, respectively [8], where $\mathbf{S}_c$ and $\mathbf{S}_u$ are task dependent selector matrices. The vector of descriptor coordinates can be reassembled as $\mathbf{q} = \mathbf{S}_c\mathbf{q}_c + \mathbf{S}_u\mathbf{q}_u$.

3. COMPUTED TORQUE CONTROL METHOD

We apply the backward Euler discretization of the DAE system and the resulting set of equations are solved by the Newton-Raphson method for the desired actuator forces and uncontrolled coordinates and Lagrangian multipliers.

We assume that the servo constraints result a $\mathbf{q}_c = \mathbf{q}_c^d$ for which the control input $\mathbf{u}$ is bounded. Considering a PD controller with gain matrices $\mathbf{K}_P$ and $\mathbf{K}_D$ the control law can be formulated as:

$$\mathbf{M}\ddot{\mathbf{q}}^d + \mathbf{\Phi}_{\mathbf{q}}^{\mathrm{T}}(\mathbf{q}^d)\boldsymbol{\lambda} = \mathbf{Q}_g + \mathbf{H}(\mathbf{q}^d)\mathbf{u} - \mathbf{K}_P(\mathbf{q}^d - \mathbf{q}) - \mathbf{K}_D(\dot{\mathbf{q}}^d - \dot{\mathbf{q}})\,, \tag{9}$$

$$\boldsymbol{\varphi}(\mathbf{q}^d) = \mathbf{0}, \tag{10}$$

where $\mathbf{q}$ is the measured and $\mathbf{q}^d$ is the desired descriptor coordinate vector. The measured value of the coordinates appears only in the linear compensator.

Introducing $\mathbf{y}^d = \dot{\mathbf{q}}^d$ we derive the first order form of equations (9-10). After the decomposition of the controlled and uncontrolled coordinates the control law can be written in the form:

ISBN 978-963-313-007-0

$$\dot{\mathbf{q}}_c^d = \mathbf{y}_c^d, \tag{11}$$

$$\dot{\mathbf{q}}_u^d = \mathbf{y}_u^d, \tag{12}$$

$$\dot{\mathbf{y}}_c^d = \mathbf{S}_c^{\mathrm{T}}\mathbf{M}^{-1}\left(-\mathbf{\Phi}_{\mathbf{q}}^{\mathrm{T}}(\mathbf{q}^d)\boldsymbol{\lambda} + \mathbf{Q}_g + \mathbf{H}(\mathbf{q}^d)\mathbf{u} - \mathbf{K}_P(\mathbf{q}^d - \mathbf{q}) - \mathbf{K}_D(\mathbf{y}^d - \dot{\mathbf{q}})\right), \tag{13}$$

$$\dot{\mathbf{y}}_u^d = \mathbf{S}_u^{\mathrm{T}}\mathbf{M}^{-1}\left(-\mathbf{\Phi}_{\mathbf{q}}^{\mathrm{T}}(\mathbf{q}^d)\boldsymbol{\lambda} + \mathbf{Q}_g + \mathbf{H}(\mathbf{q}^d)\mathbf{u} - \mathbf{K}_P(\mathbf{q}^d - \mathbf{q}) - \mathbf{K}_D(\mathbf{y}^d - \dot{\mathbf{q}})\right), \tag{14}$$

$$\boldsymbol{\varphi}(\mathbf{q}^d) = \mathbf{0}. \tag{15}$$

Equation (11) is identity thus we can leave it out of consideration. Equation (12-15) can be discretized by backward Euler method:

$$\frac{\mathbf{q}_{u,i+1}^d - \mathbf{q}_{u,i}^d}{h} = \mathbf{y}_{u,i+1}^d, \tag{16}$$

$$\frac{\mathbf{y}_{u,i+1}^d - \mathbf{y}_{u,i}^d}{h} = \mathbf{S}_u^{\mathrm{T}}\mathbf{M}^{-1}\left(-\mathbf{\Phi}_{\mathbf{q}}^{\mathrm{T}}(\mathbf{q}_{i+1}^d)\boldsymbol{\lambda}_{i+1} + \mathbf{Q}_g + \mathbf{H}(\mathbf{q}_{i+1}^d)\mathbf{u}_{i+1} - \mathbf{K}_P(\mathbf{q}_{i+1}^d - \mathbf{q}_{i+1}) - \mathbf{K}_D(\mathbf{y}_{i+1}^d - \dot{\mathbf{q}}_{i+1})\right), \tag{17}$$

$$\mathbf{0} = -\dot{\mathbf{y}}_{c,i+1}^d + \mathbf{S}_c^{\mathrm{T}}\mathbf{M}^{-1}\left(-\mathbf{\Phi}_{\mathbf{q}}^{\mathrm{T}}(\mathbf{q}_{i+1}^d)\boldsymbol{\lambda}_{i+1} + \mathbf{Q}_g + \mathbf{H}(\mathbf{q}_{i+1}^d)\mathbf{u}_{i+1} - \mathbf{K}_P(\mathbf{q}_{i+1}^d - \mathbf{q}_{i+1}) - \mathbf{K}_D(\mathbf{y}_{i+1}^d - \dot{\mathbf{q}}_{i+1})\right), \tag{18}$$

$$\mathbf{0} = \boldsymbol{\varphi}(\mathbf{q}_{i+1}^d). \tag{19}$$

Equations (16-19) constitute a system of $2n-l+m$ number of nonlinear equations for the $(i+1)^{\text{th}}$ value of the desired uncontrolled coordinates $\mathbf{q}_{u,i+1}^d$, their time derivatives $\mathbf{y}_{u,i+1}^d$, the control inputs $\mathbf{u}_{i+1}$ and the Lagrange multipliers $\boldsymbol{\lambda}_{i+1}$. It can be formulated as a function $\mathbf{F}_{i+1}$ of the vector of unknowns $\mathbf{z} = [\mathbf{q}_{u,i+1}^d \quad \mathbf{y}_{u,i+1}^d \quad \mathbf{u}_{i+1} \quad \boldsymbol{\lambda}_{i+1}]^{\mathrm{T}}$ as follows:

$$\mathbf{F}_{i+1} = \begin{bmatrix} \mathbf{q}_{u,i+1}^d - \mathbf{q}_{u,i}^d - h\mathbf{y}_{u,i+1}^d \\ \mathbf{y}_{u,i+1}^d - \mathbf{y}_{u,i}^d - h\mathbf{S}_u^{\mathrm{T}}\mathbf{M}^{-1}\left(-\mathbf{\Phi}_{\mathbf{q}}^{\mathrm{T}}(\mathbf{q}_{i+1}^d)\boldsymbol{\lambda}_{i+1} + \mathbf{Q}_g + \mathbf{H}(\mathbf{q}_{i+1}^d)\mathbf{u}_{i+1} - \mathbf{K}_P(\mathbf{q}_{i+1}^d - \mathbf{q}_{i+1}) - \mathbf{K}_D(\mathbf{y}_{i+1}^d - \dot{\mathbf{q}}_{i+1})\right) \\ \dot{\mathbf{y}}_{c,i+1}^d - \mathbf{S}_c^{\mathrm{T}}\mathbf{M}^{-1}\left(-\mathbf{\Phi}_{\mathbf{q}}^{\mathrm{T}}(\mathbf{q}_{i+1}^d)\boldsymbol{\lambda}_{i+1} + \mathbf{Q}_g + \mathbf{H}(\mathbf{q}_{i+1}^d)\mathbf{u}_{i+1} - \mathbf{K}_P(\mathbf{q}_{i+1}^d - \mathbf{q}_{i+1}) - \mathbf{K}_D(\mathbf{y}_{i+1}^d - \dot{\mathbf{q}}_{i+1})\right) \\ \boldsymbol{\varphi}(\mathbf{q}_{i+1}^d) \end{bmatrix}. \tag{20}$$

The system of nonlinear equations is solved by Newton-Raphson method in the form $\mathbf{J}_{i+1}(\mathbf{z}_{i+1} - \mathbf{z}_i) = -\mathbf{F}_{i+1}$. The Jacobian is the following:

$$\mathbf{J}_{n+1} = \begin{bmatrix} \mathbf{I} & -h\mathbf{I} & \mathbf{0} & \mathbf{0} \\ h\mathbf{S}_u^{\mathrm{T}}\mathbf{M}^{-1}\left(\dfrac{\partial(\mathbf{\Phi}_{\mathbf{q}}^{\mathrm{T}}\boldsymbol{\lambda} - \mathbf{H}\mathbf{u})}{\partial \mathbf{q}_u^d} + \mathbf{K}_P\mathbf{S}_u\right) & \mathbf{I} + h\mathbf{S}_u^{\mathrm{T}}\mathbf{M}^{-1}\mathbf{K}_D\mathbf{S}_u & -h\mathbf{S}_u^{\mathrm{T}}\mathbf{M}^{-1}\mathbf{H} & h\mathbf{S}_u^{\mathrm{T}}\mathbf{M}^{-1}\mathbf{\Phi}_{\mathbf{q}}^{\mathrm{T}} \\ \mathbf{S}_c^{\mathrm{T}}\mathbf{M}^{-1}\left(\dfrac{\partial(\mathbf{\Phi}_{\mathbf{q}}^{\mathrm{T}}\boldsymbol{\lambda} - \mathbf{H}\mathbf{u})}{\partial \mathbf{q}_u^d} + \mathbf{K}_P\mathbf{S}_u\right) & \mathbf{S}_c^{\mathrm{T}}\mathbf{M}^{-1}\mathbf{K}_D\mathbf{S}_u & -\mathbf{S}_c^{\mathrm{T}}\mathbf{M}^{-1}\mathbf{H} & \mathbf{S}_c^{\mathrm{T}}\mathbf{M}^{-1}\mathbf{\Phi}_{\mathbf{q}}^{\mathrm{T}} \\ \mathbf{\Phi}_{\mathbf{q}}\mathbf{S}_u & \mathbf{0} & \mathbf{0} & \mathbf{0} \end{bmatrix}. \tag{21}$$

In some cases the Jacobian matrix may be ill-conditioned, but the problem can be handled by singular value decomposition where we leave out the relatively small elements.

4. SIMULATIONS AND COMPARARISON WITH SEMI-ANALYTICAL RESULTS

The pole cart model is examined with the present computed torque method. The mechanical model can be seen in Fig.2. left and middle. This system is the most reduced model of any crane system and the ACROBOTER robot. The system is described by the redundant set of descriptor coordinates $\mathbf{q} = [x_1 \quad x_2 \quad z_2]^{\mathrm{T}}$. The geometric constraint vector is $\boldsymbol{\varphi}(\mathbf{q}) = 0.5[(x_2 - \mathrm{x}_1)^2 + z_2^2 - L^2]$, which means that the pole has a constant length L. The equation of motion is written in the form of (5) and (6):

$$\begin{bmatrix} m_1 & 0 & 0 \\ 0 & m_2 & 0 \\ 0 & 0 & m_2 \end{bmatrix}\begin{bmatrix} \ddot{x}_1 \\ \ddot{x}_2 \\ \ddot{z}_2 \end{bmatrix} + \begin{bmatrix} x_1 - x_2 \\ -x_1 + x_2 \\ z_2 \end{bmatrix}[\lambda_1] = \begin{bmatrix} 0 \\ 0 \\ -m_2 g \end{bmatrix} + \begin{bmatrix} 1 \\ 0 \\ 0 \end{bmatrix}[F_1], \tag{22}$$

$$\tfrac{1}{2}[(x_2 - \mathrm{x}_1)^2 + z_2^2 - L^2] = [0]. \tag{23}$$

ISBN 978-963-313-007-0

According to equation (8) the servo constraint vector is composed by the functions $\mathbf{h}(\mathbf{q}) = [x_2]$ and $\mathbf{p}(t) = [x_2^d]$, so the servo constraint reads the form:

$$x_2 - x_2^d = 0, \tag{24}$$

from which we can see that the servo constraint can be solved for the controlled coordinate $x_2 = x_2^d$ and can be substituted into the control law (9).

The desired uncontrolled coordinate values x_1 and z_2, the Lagrangian multiplicator λ_1 and the desired force F_1 are calculated by the backward Euler algorithm. The parallel simulation of the controlled dynamical system must be done at the same time because the linear compensator calculates a position and a velocity error $\mathbf{q}^d - \mathbf{q}$ and $\dot{\mathbf{q}}^d - \dot{\mathbf{q}}$. The simulation was accomplished with the Baumgarte stabilization of the equation of motion [1], which can be written as follows if the geometric constraints not depend on time explicitly:

$$\begin{bmatrix} \mathbf{M} & \mathbf{\Phi}_q^{\mathrm{T}} \\ \mathbf{\Phi}_q & \mathbf{0} \end{bmatrix} \begin{bmatrix} \ddot{\mathbf{q}} \\ \boldsymbol{\lambda} \end{bmatrix} = \begin{bmatrix} \mathbf{Q} \\ -\dot{\mathbf{\Phi}}_q \dot{\mathbf{q}} - 2\alpha \mathbf{\Phi}_q \dot{\mathbf{q}} - \beta^2 \boldsymbol{\varphi} \end{bmatrix}. \tag{25}$$

In order to verify the simulations the inverse dynamical calculation was accomplished by semi-analytical way. In this calculation the minimum set of descriptor coordinates was used: $\overline{\mathbf{q}} = [\mathrm{x}_1 \quad \psi]^{\mathrm{T}}$, see Fig.2. The equations of motion derived from the Lagrange equation of the second kind.

$$(m_1 + m_2)\ddot{x}_1 + Lm_2 \cos(\psi)\ddot{\psi} - Lm_2 \sin(\psi)\dot{\psi}^2 = F_1, \tag{26}$$

$$\cos(\psi)\ddot{x}_1 + L\ddot{\psi} + g\sin(\psi) = 0. \tag{27}$$

The task is defined by the servo constraint with the functions $\mathbf{h}(\overline{\mathbf{q}}) = [x_1 + L\sin(\psi)]$ and $\mathbf{p}(t) = [x_2^d]$. The servo constraint can be written as follows:

$$x_1 + L\sin(\psi) - x_2^d = 0. \tag{28}$$

The servo constraint equation can be solved for the angle ψ and can be substituted into equations of motion (26) and (27). Equation (27) gives a second order differential equation for x_1 and its solution gives the desired position x_1 of the cart. After that the desired control force control can be determined by equation (26).

We mention that the differential equation (27) is singular at the vertical position of the pole, when $x_1 - x_2^d = 0$. In this configuration the coefficient $c_1(x_1, x_2^d, \dot{x}_1, \dot{x}_2^d)$ of $\ddot{x}_1$ is zero. But the equation still can be solved if we choose a small number ε and introduce the modified coefficient of $\ddot{x}_1$ as $\tilde{c}_1 = 2(H(c_1) - 1)\max(\mathrm{abs}(c_1, \varepsilon))$, where $H(c_1)$ is the unit step function and $H(c_1) = 0$ if $c_1 < 0$ and $H(c_1) = 1$ if $c_1 \geq 0$. The $\tilde{c}_1$ coefficient is shown in Fig.2. right. This modification of the differential equation (27) causes small amplitude high frequency oscillation in the x_1 solution. This oscillation is amplified in the control force F_1, but this oscillation can be filtered from the signal. The semi-analytically calculated desired value of x_1 can be seen in Fig.3./a and Fig.4./a denoted by `x1an`. The corresponding desired control input F_1 and its the filtered version is shown in Fig.3./h and Fig.4./h denoted by `F1an` and `F1an.s` respectively.

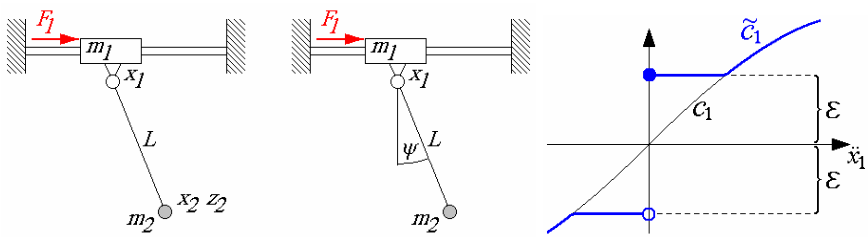

Fig.2. Left: pole cart model with redundant set of descriptor coordinates, middle: minimum set of descriptor coordinates. Right: coefficient of $\ddot{x}_1$.

The desired trajectory must be at least four times continuously differentiable because the analytical investigations shows that the control force F_1 depends on the fourth time derivative of the desired coordinate x_2^d. In other words the relative degree is 4 [2]. Because of

7th International Conference on Mechanical Engineering 2010 (Gépészet 2010)
Budapest, 25-26. May 2010.
ISBN 978-963-313-007-0

this, the desired trajectory is based on the $\arctan(t)$ function as it has infinite number of time derivative. The simulation results can be seen in Fig.3. and Fig.4. The simulation that is shown in Fig.4. considered the saturation of the control force F_1.

The physical parameters of the simulation was $g = 9.81[\text{m/s}^2]$, $m_1 = 1[\text{kg}]$, $m_2 = 1[\text{kg}]$ $L = 1[\text{m}]$. The gain matrices of the linear compensator was set to be $\mathbf{K}_P = diag[8,\ 0.8,\ 0.8][\text{N/m}]$ and $\mathbf{K}_D = diag[20,\ 4,\ 4][\text{Ns/m}]$. The parameters of the Baumgarte stabilization method was $\alpha = 5$ and $\beta = 5$, which provided the stability of the constraint equation during the simulation of the investigated dynamical system.

The semi-analytically calculated uncontrolled desired coordinate x_1^d and its desired value given by the computed torque control algorithm are shown in Fig.3./a and Fig.4./a and denoted by `x1an` and `x1d` respectively. If the control force F_1 is not bounded than the two results is very close to each other. In the case of saturated control force the deviation between the analytical and the simulated result is significant, but the simulated x_1^d converges to the analytical after a few oscillations. Fig.3./b and Fig.4./b show the desired value of x_1 and x_2 given by the controller and they are denoted by `x1d` and `x2d` respectively. The simulation of the pole-cart system gives `x1sim` and `x2sim`. The error between the desired and the simulated values is shown in Fig.3./e and Fig.4./e and denoted by `x1err` and `x2err`. The maximum value of the error of the controlled coordinate x_2 is 5mm if the control force is not bounded and 100mm if F_1 saturates. The maximal error strongly depends on the gain matrices $\mathbf{K}_P$ and $\mathbf{K}_D$, however the gains cannot be set above a definite value because of stability problems. The desired and simulated value of z_2 can be seen in Fig.3./c and Fig.4./c, and the error is shown in Fig.3./e and Fig.4./e, the notation is `z2d`, `z2sim` and `z2err`.

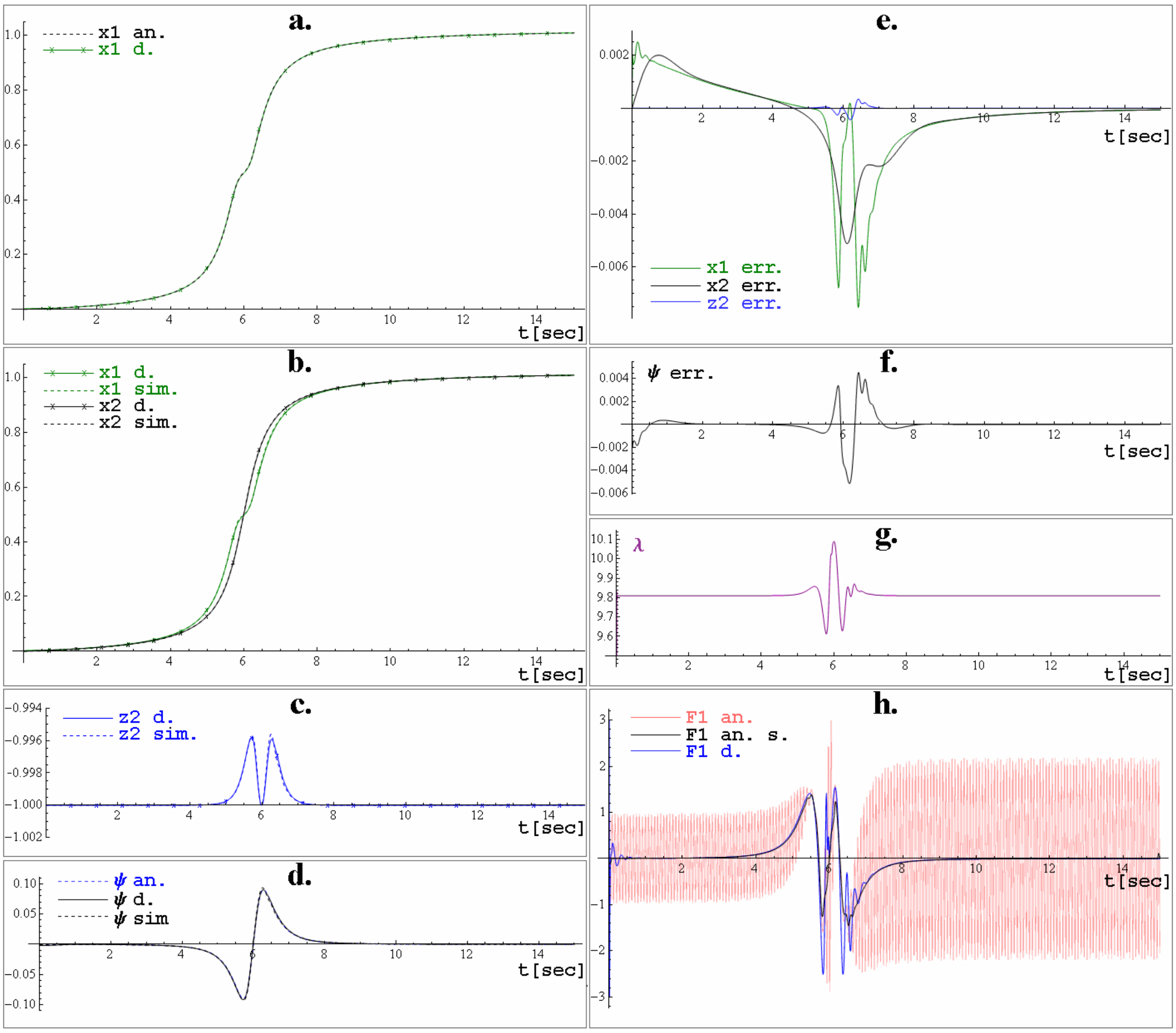

Fig.3. Simulation results

7th International Conference on Mechanical Engineering 2010 (Gépészet 2010)
Budapest, 25-26. May 2010.
ISBN 978-963-313-007-0

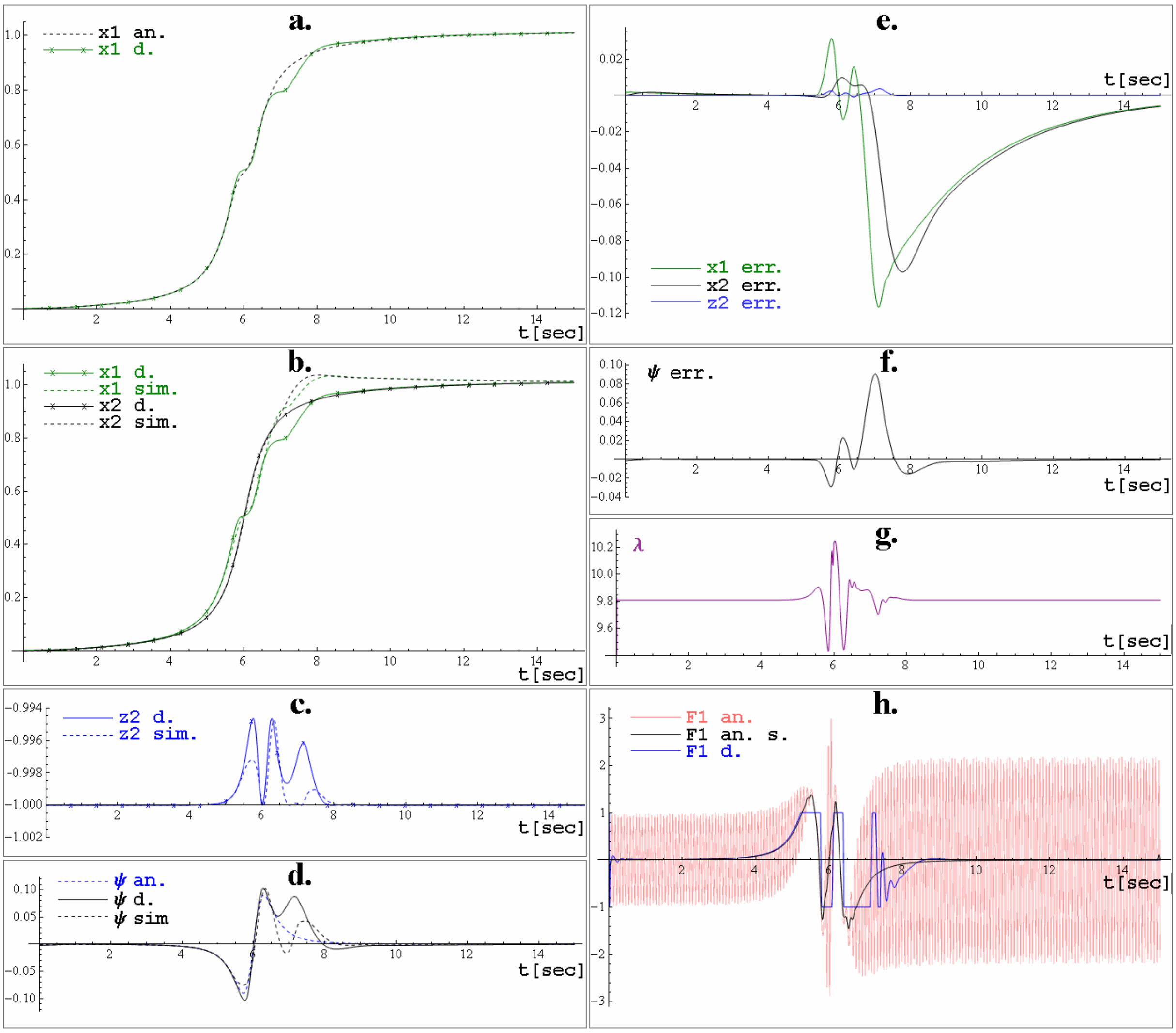

Fig.4. Simulation results in the case of saturated control input

In order to have a better imagination of the motion the angle of the pole is plotted in Fig.3./d and Fig.4./d. The analytically calculated desired value of ψ is denoted by ψan, the desired value generated by the controller is denoted by ψd and the simulated motion is ψsim. The differences between of the three functions are significant only in the case of saturated F_1. The error between the desired and the simulated ψ angle is shown in Fig.3./f and Fig.4./f. The desired Lagrange multiplicator is shown in Fig.3./g and Fig.4./g. Fig.3./h and Fig.4./h. show the control force F_1. F1an denotes the result of the semi-analytical calculation and F1an.s is the same signal after processed by a digital filter algorithm. We can see that the oscillation of the unfiltered signal has a very definite frequency and can be filtered out very efficiently. In the case of unbounded F_1 the desired control force calculated by the controller oscillates in the appearance of fast desired motions around $t = 6[\text{s}]$, but the oscillations are suppressed and the force signal converges to the semi-analytically calculated curve. In the case of the saturated control force the deviation from the semi-analytical signal is much larger and has some delay, but after a short time it converges to the semi-analytical curve.

Summarizing, the diagrams in both Fig.3. and Fig.4. shows that the results given by the computed torque control with backward Euler discretization gives feasible control inputs, suppresses the error of the controlled coordinate, and the results are in strong connection with the semi-analytical results.

ISBN 978-963-313-007-0

5. CONCLUSION

A formalism was proposed for the computed torque control of under-actuated and natural coordinate based dynamical systems. The numerical simulations showed the applicability of the algorithm. The simulation also showed that the method gives the same results as the analytical solution of the inverse dynamic problem.

Our studies indicated that in case of more complex and larger systems the Jacobian matrix may be ill conditioned. The examination of this problem is a future work.

The feasibility of the present control approach is planned to be tested in the framework of the ACROBOTER project.

ACKNOWLEDGEMENTS

This work was supported in part by the Hungarian National Science Foundation under grant no. OTKA K068910, the ACROBOTER (IST-2006-045530) project, the Hungarian Academy of Sciences under grant no. MTA-NSF/103, and by the HAS-BME Research Group on Dynamics of Machines and Vehicles.

REFERENCES

Books:

[1] de Jalón J. G., Bayo E. *Kinematic and dynamic simulation of Multibody systems: the real-time chalenge.* Springer-Verlag, 1994.

[2] Isidori A. *Nonlinear Control Systems – An Introduction*. Springer-Verlag, 1989.

Journals:

[3] Blajer W. Kołodziejczyk K. *Modeling of Underactuated Mechanical Systems in Partly Specified Motion.* Journal of Theoretical and Applied Mechanics, 2008;46(2):383-394.

[4] Stépán G., Toth A., Kovacs L. L., Bolmsjö G., Nikoleris G., Surdilovic D., Conrad A., Gasteratos A., Kyriakoulis N., Chrysostomou D., Kouskouridas R., Canou J., Smith T., Harwin W., Loureiro R., Lopez R., Moreno M. A Ceiling Based Crawling, Hoisting and Swinging Service Robot Platform, In Proceedings of Beyond Gray Droids: Domestic Robot Design for the 21st Century Workshop at HCI 2009. In press, 2009.

[5] Kövecses J., Piedoboeuf J.-C., Lange C. Dynamic Modeling and Simulation of Constrained Robotic Systems. IEEE/ASME Transactions on Mechatronics 2003;8(2):165-177.

Conference proceedings:

[6] Blajer W., Dziewiecki K., Kołodziejczyk K., Mazur Z. Inverse Dynamics of a Two-Degree-of-Freedom Underactuated System: Analysis and Experiment. 10th Conference on Dynamical Systems - Theory and Applications DSTA-2009, December 7-10 Łódź, Poland.

[7] Zelei A., Kovács L. L., Stépán G. Computed Torque Control Method For Under-Actuated Manipulator. In: Proceedings of the ASME 2009 International Design Engineering Technical Conferences & Computers and Information in Engineering Conference, San Diego, California, USA, 2009. Paper DETC2009-86409.

PhD dissertations:

[8] Lammerts I. M. M. Adaptive Computed Reference Computed Torque Control. Eindhoven university of technology, 1993.